


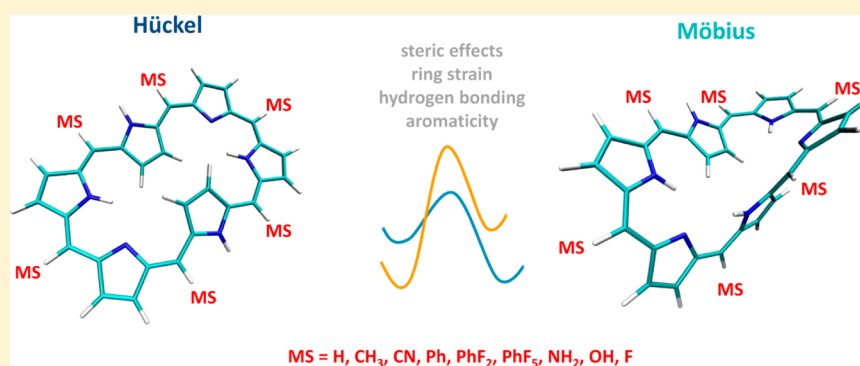
# Effect of the Meso-Substituent in the Hückel-to-Möbius Topological Switches

Enrique Marcos,<sup>\*,†,‡</sup> Josep M. Anglada,<sup>†</sup> and Miquel Torrent-Sucarrat<sup>\*,†</sup>

<sup>†</sup>Departament de Química Biològica i Modelització Molecular, Institut de Química Avançada de Catalunya (IQAC-CSIC), c/Jordi Girona 18, E-08034 Barcelona, Spain

<sup>‡</sup>Department of Biochemistry, University of Washington, Seattle, Washington 98195, United States

 Supporting Information



**ABSTRACT:** Expanded porphyrins have emerged as a new promising class of molecules for the creation of new Hückel-to-Möbius topological switches with distinct aromaticities and magnetic and electric properties. In this work, we report a theoretical investigation of the conformational switch between the Hückel planar and the singly twisted Möbius structure for eight different meso-substituted [28]-hexaphyrins (with different steric effects and electron-withdrawing and -releasing character). Our results show how a change in the nature of the meso-substituent is able to turn an endothermic interconversion process with a high energy barrier into an exothermic and almost barrierless Hückel–Möbius transition. We also provide a thorough analysis of the main factors (aromaticity, intramolecular hydrogen bonds, ring strain, and steric effects) that play a role in this interconversion process. Overall, these results are very relevant to find new ways to control the thermochemistry and kinetics of these topological switches and even “freeze” the switch in the desired Möbius or Hückel conformation.

## INTRODUCTION

Expanded porphyrins have attracted considerable attention owing to their particular multimetal coordination, optical, magnetic, and electric properties, and structural versatility. In recent years, significant efforts have been devoted to the synthesis of new expanded porphyrins.<sup>1</sup> Moreover, expanded porphyrins have emerged as a new promising class of molecules for creation of Hückel-to-Möbius topological switches.<sup>2</sup> The conformational flexibility, the number, the position, and the type of substituents on the pyrrolic and meso positions and metalation of the porphyrins allow them to acquire different structures with distinct aromaticities and nonlinear optical properties.<sup>3</sup> Several expanded porphyrins with different Hückel and Möbius topologies have been prepared through replacement of the solvent and protonation,<sup>4</sup> temperature control,<sup>5–7</sup> metal coordination,<sup>8</sup> and functional group modifications.<sup>9</sup>

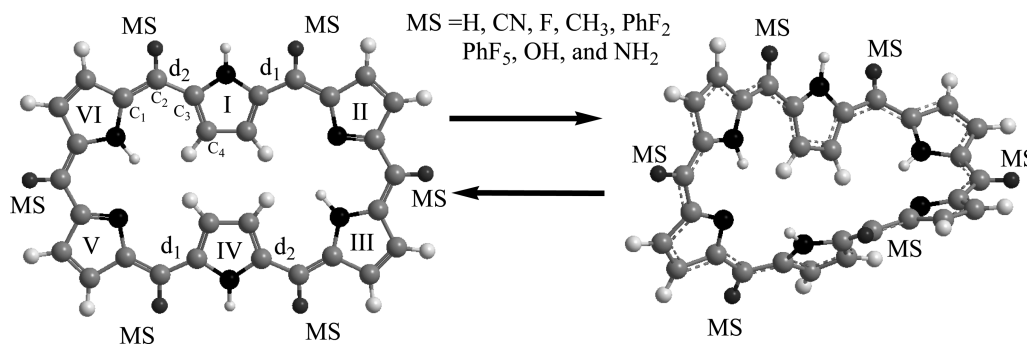
In the literature, there have been several studies comparing Hückel and Möbius isomers of annulenes and probing mechanisms of their interconversions,<sup>10,11</sup> but only a few computational studies for expanded porphyrins have been reported. In a very recent paper,<sup>12</sup> the present authors reported

the reaction mechanism between the Hückel planar and the singly twisted Möbius structures for two different meso-substituted [28]hexaphyrins(1.1.1.1.1.1) using different computational methodologies; i.e., the meso-substituents studied were the hydrogen atoms and pentafluorophenyl groups. We showed that the nature of the meso-substituent can have an important effect in the thermochemistry and kinetics of these topological switches. Moreover, the obtained results of relative free energies in THF solvent for the pentafluorophenyl meso-substituents are in reasonable agreement with the experimental estimation of the activation energy of  $8 \pm 1$  kcal·mol<sup>-1</sup> for the interconversion between the Möbius and Hückel structures.<sup>6</sup> It is worth noting that Alonso and co-workers<sup>13</sup> also studied this interconversion process for the [26]- and [28]hexaphyrins using the hydrogen atom as meso-substituent at the B3LYP/6-31G(d,p) level of theory. Their reported results are in reasonable agreement with our previous work.<sup>12</sup> Moreover, Alonso and co-workers<sup>14</sup> recently reported a computational

Received: March 13, 2014

Published: May 9, 2014

**Scheme 1. Switching Topology Scheme between Planar Hückel Antiaromatic and Möbius Aromatic Conformers of the Meso-Substituted [28]Hexaphyrins(1.1.1.1.1.1) for the Eight Meso-Substituents Considered in This Work**



study of the topological switching in [32]heptaphyrins(1.1.1.1.1.1) between different figure eight, Möbius, and untwisted conformations.

In this paper, we report a theoretical investigation of the conformational switch between Hückel and Möbius structures for eight [28]hexaphyrins with different meso-substituents (hydrogen (H), cyano (CN), fluorine (F), methyl (CH<sub>3</sub>), 2,6-fluorophenyl (PhF<sub>2</sub>), pentafluorophenyl (PhF<sub>5</sub>), hydroxyl (OH), and amino (NH<sub>2</sub>),<sup>15</sup> see Scheme 1), possessing different steric effects and electron-withdrawing and -releasing characters. Moreover, we have analyzed the different factors (aromaticity, intramolecular hydrogen bonds, ring strain, and steric effects) that play a role in the interconversion processes. These results are very relevant in order to find new ways to control the thermochemistry and kinetics of these topological switches, in such a way that it would be possible to “freeze” the switch in the desired Möbius or Hückel conformation. It is worth noting that the meso-substituents considered in this work have been chosen for an academic purpose to illustrate the relevance of several factors in this interconversion process. Although some of these models could be considered “unrealistic” from an experimental point of view, their study allows us to be systematic in understanding the nature of the hexaphyrin switch. The present study aims at characterizing the behavior of the Möbius–Hückel conformational switch with the ultimate goal of providing the experimental research groups that work in this field a rigorous framework to rationalize past experimental results and design future experiments.

## ■ COMPUTATIONAL METHODS

In our previous work,<sup>12</sup> we benchmarked a variety of computational methods to describe the Hückel-to-Möbius interconversion mechanism. The calculations were performed with the B3LYP, BH&HLYP, CAM-B3LYP, M05-2X, and MP2 methodologies along with the 6-31G and 6-311G(d,p) basis sets. For benchmarking purposes, single-point energies were also calculated at the CCSD(T)/6-31G level of theory. These benchmark calculations were very valuable in order to establish the most appropriate theoretical approach capable of providing reliable results. Our calculations showed that the increment of the basis set from 6-31G to 6-311G(d,p) results in small variations of the relative stabilities and energy barriers. On the other hand, we realized that the selection of a method that simultaneously describes the relative stability and the energy barrier of the interconversion process between Hückel and Möbius structures is a complex task. For instance, we pointed out the bad performances of the B3LYP and MP2 methodologies, which tend to exaggerate the delocalization of the conjugated Möbius systems and overstabilize their structures, in agreement with previous studies reported in the literature.<sup>11,16</sup> Based on this benchmark, our results provided evidence that the CAM-B3LYP and M05-2X are the functionals giving the most equilibrated

results for the different interconversion steps of these topological switches. Then, we chose the M05-2X<sup>17</sup> method, along with the 6-311G(d,p) basis set,<sup>18</sup> to optimize the stationary points of the interconversion mechanisms for the eight different meso-substituted [28]hexaphyrins(1.1.1.1.1.1) investigated here. At this level of theory, we have also calculated the harmonic vibrational frequencies to verify the nature of the corresponding stationary points (minimum or transition state) and provided the zero-point vibrational energy (ZPE) and the thermodynamic contributions to the enthalpy and free energy for  $T = 298$  K. The X-ray structures available for the Möbius and Hückel structures of the PhF<sub>5</sub> model have been used as the initial geometry,<sup>5</sup> and no symmetry restrictions have been considered in the optimization processes. All the energetic increments discussed in the text are energy plus ZPE values. The aromaticity of selected structures has been evaluated using a geometric (harmonic oscillator model of aromaticity, HOMA)<sup>19</sup> and magnetic (nucleus-independent chemical shift, NICS,<sup>20</sup> using the GIAO method at the M05-2X/6-311G(d,p) level) criteria. All geometries, frequencies, and energies were calculated using the Gaussian09 program package.<sup>21</sup>

The fuzzy atom bond orders (FBO)<sup>22</sup> and fuzzy atomic charges using the atomic definition of the Becke–rho<sup>23</sup> scheme<sup>24</sup> have been evaluated with the FUZZY program.<sup>25</sup> The charge distribution was also obtained following the natural bond orbital (NBO) partitioning scheme by Weinhold and co-workers.<sup>26</sup> To assess the contributions of steric effects and both electrostatic and orbital interactions to the relative stability between Hückel and Möbius species, we performed an energy decomposition analysis (EDA),<sup>27</sup> employing basic atoms as fragments to decompose the interaction energy. We have used the EDA implementation in the ADF (2012.01) program package<sup>28</sup> along with the BH&HLYP<sup>29</sup> functional and TZP basis set.<sup>30</sup>

The main difficulty in finding the transition state (TS) connecting the Hückel-like and Möbius-like structures lies in the definition of a reaction coordinate. This is due to the fact that this transition not only involves a rotation of the central pyrrole rings but also involves a reorganization of the other pyrrole rings. For this reason, we have employed the nudged elastic band (NEB) method<sup>31</sup> to build a model for the complete reaction pathway and we have taken the maximum points of this model for the search of the corresponding transition states. We have used the NEB method implemented in pDynamo<sup>32</sup> program, in conjunction with the PM6 semiempirical method<sup>33</sup> for this purpose.

## ■ RESULTS AND DISCUSSION

**Switching Mechanisms between Hückel and Möbius Conformations.** Scheme 1 shows that the switching process between Hückel and Möbius structures mainly implies the rotation around the carbon–carbon bonds ( $d_1$  and  $d_2$ ) of the meso bridges attached to the pyrrole units labeled as I and IV (notice that both rings are equivalent by symmetry). Herein, we refer to the pathways of the interconversion between Hückel and Möbius topologies through rotations of  $d_1$  and  $d_2$  bonds as mechanisms A and B, respectively. The relative energies,

**Table 1. Relative Energies, Energies plus Zero-Point Energies, Enthalpies, and Free Energies of the Hückel → Möbius Switch for Four Meso-Substituents (H, CN, F, and CH<sub>3</sub>) Studied in this Work via the Two Mechanisms (A and B) Evaluated at the M05-2X/6-311G(d,p) Level<sup>a</sup>**

subst	species	mechanism A				species	mechanism B			
		$\Delta E$	$\Delta(E+ZPE)$	$\Delta H$	$\Delta G$		$\Delta E$	$\Delta(E+ZPE)$	$\Delta H$	$\Delta G$
H	H <sub>1</sub>	0.00	0.00	0.00	0.00	H <sub>1</sub>	0.00	0.00	0.00	0.00
	TS <sub>1A</sub>	10.89	10.25	9.81	10.97	TS <sub>1B</sub>	7.39	6.93	6.48	7.70
	M <sub>1A</sub>	4.69	4.11	3.89	4.71	M <sub>1B</sub>	5.65	4.97	4.85	5.23
	TS <sub>2A</sub>	10.97	7.24	6.78	8.02	TS <sub>2B</sub>	13.07	9.47	8.94	10.46
	M <sub>2</sub>	2.49	1.99	1.78	2.56	M <sub>2</sub>	2.49	1.99	1.78	2.56
CN	H <sub>1</sub>	0.00	0.00	0.00	0.00	H <sub>1</sub>	0.00	0.00	0.00	0.00
	TS <sub>1A</sub>	8.66	8.16	7.72	9.32	TS <sub>1B</sub>	6.16	5.75	5.36	6.50
	M <sub>1A</sub>	3.92	3.06	3.11	3.21	M <sub>1B</sub>	4.56	3.73	3.83	3.59
	TS <sub>2A</sub>	10.13	6.34	6.13	6.75	TS <sub>2B</sub>	12.23	8.42	8.17	8.95
	M <sub>2</sub>	1.65	1.04	1.07	1.20	M <sub>2</sub>	1.65	1.04	1.07	1.20
F	H <sub>1</sub>	0.00	0.00	0.00	0.00	H <sub>1</sub>	0.00	0.00	0.00	0.00
	TS <sub>1A</sub>	12.95	12.51	12.10	13.21	TS <sub>1B</sub>	9.73	9.29	8.89	9.81
	M <sub>1A</sub>	8.68	8.22	8.16	8.44	M <sub>1B</sub>	9.11	8.52	8.54	8.22
	TS <sub>2A</sub>	15.90	12.10	11.79	12.51	TS <sub>2B</sub>	18.00	14.56	14.13	15.29
	M <sub>2</sub>	7.20	6.76	6.69	6.90	M <sub>2</sub>	7.20	6.76	6.69	6.90
CH <sub>3</sub>	H <sub>1</sub>	0.00	0.00	0.00	0.00	H <sub>1</sub>	0.00	0.00	0.00	0.00
	TS <sub>1A</sub>	5.07	3.60	3.33	5.04	TS <sub>1B</sub>	1.82	0.74	-0.17	3.85
	M <sub>1A</sub>	-5.87	-7.93	-7.73	-6.85	M <sub>1B</sub>	-4.18	-6.16	-5.97	-5.26
	TS <sub>2A</sub>	-1.71	-6.54	-6.37	-5.99	TS <sub>2B</sub>	0.76	-4.18	-3.98	-3.45
	M <sub>2</sub>	-7.96	-9.88	-9.62	-9.14	M <sub>2</sub>	-7.96	-9.88	-9.62	-9.14

<sup>a</sup>All quantities are in kcal·mol<sup>-1</sup> and  $T = 298$  K.

**Table 2. Relative Energies, Energies plus Zero Point Energies, Enthalpies, and Free Energies for the Hückel → Möbius Switch for Four Meso-Substituents (PhF<sub>2</sub>, PhF<sub>3</sub>, OH, and NH<sub>2</sub>) Studied in This Work via the Two Mechanisms (A and B) Evaluated at the M05-2X/6-311G(d,p) Level<sup>a</sup>**

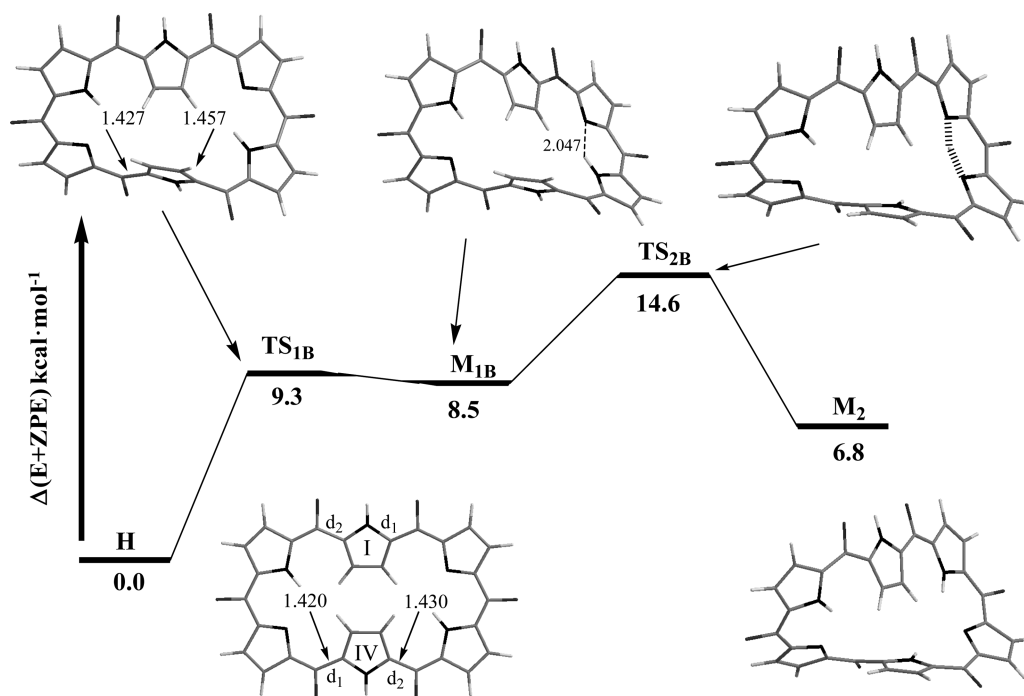
subst	species	mechanism A				species	mechanism B			
		$\Delta E$	$\Delta(E+ZPE)$	$\Delta H$	$\Delta G$		$\Delta E$	$\Delta(E+ZPE)$	$\Delta H$	$\Delta G$
PhF <sub>2</sub>	H <sub>1</sub>	0.00	0.00	0.00	0.00	H <sub>1</sub>	0.00	0.00	0.00	0.00
	TS <sub>1A</sub>	7.85	7.67	7.11	8.94	TS <sub>1B</sub>	5.31	4.85	4.38	6.38
	M <sub>1A</sub>	3.30	2.28	2.30	2.18	M <sub>1B</sub>	3.67	3.05	3.06	3.36
	TS <sub>2A</sub>	10.38	6.44	6.19	6.58	TS <sub>2B</sub>	11.47	7.64	7.33	8.29
	M <sub>2</sub>	0.04	-0.51	-0.53	-1.23	M <sub>2</sub>	0.04	-0.51	-0.53	-1.23
PhF <sub>3</sub>	H <sub>1</sub>	0.00	0.00	0.00	0.00	H <sub>1</sub>	0.00	0.00	0.00	0.00
	TS <sub>1A</sub>	5.52	4.83	4.34	5.60	TS <sub>1B</sub>	3.98	3.42	3.00	4.25
	M <sub>1A</sub>	3.10	2.06	2.12	1.60	M <sub>1B</sub>	2.62	2.03	2.08	1.31
	TS <sub>2A</sub>	7.92	4.03	3.79	4.14	TS <sub>2B</sub>	10.06	5.92	5.91	4.37
	M <sub>2</sub>	-0.63	-1.51	-1.87	-1.95	M <sub>2</sub>	-0.63	-1.51	-1.87	-1.95
OH	H <sub>1</sub>	0.00	0.00	0.00	0.00	H <sub>1</sub>	0.00	0.00	0.00	0.00
	TS <sub>1A</sub>	17.40	16.47	16.27	16.95	TS <sub>1B</sub>	14.55	13.25	13.36	12.78
	M <sub>1A</sub>	3.24	2.69	2.72	2.75	M <sub>1B</sub>	5.15	4.77	4.89	4.91
	TS <sub>2A</sub>	10.37	6.63	6.57	6.98	TS <sub>2B</sub>	13.51	9.68	9.62	9.99
	M <sub>2</sub>	4.09	3.35	3.50	3.40	M <sub>2</sub>	4.09	3.35	3.50	3.40
NH <sub>2</sub>	H <sub>1</sub>	0.00	0.00	0.00	0.00	H <sub>1</sub>	0.00	0.00	0.00	0.00
	TS <sub>1A</sub>	12.53	12.03	11.75	12.81	TS <sub>1B</sub>	13.10	12.89	12.66	13.29
	M <sub>1A</sub>	-1.91	-3.35	-2.92	-3.39	M <sub>1B</sub>	-0.25	-1.69	-1.14	-1.89
	TS <sub>2A</sub>	5.48	1.29	1.45	1.68	TS <sub>2B</sub>	7.92	3.43	3.76	3.44
	M <sub>2</sub>	-1.58	-2.58	-2.28	-2.54	M <sub>2</sub>	-1.58	-2.58	-2.28	-2.54

<sup>a</sup>All quantities are in kcal·mol<sup>-1</sup> and  $T = 298$  K.

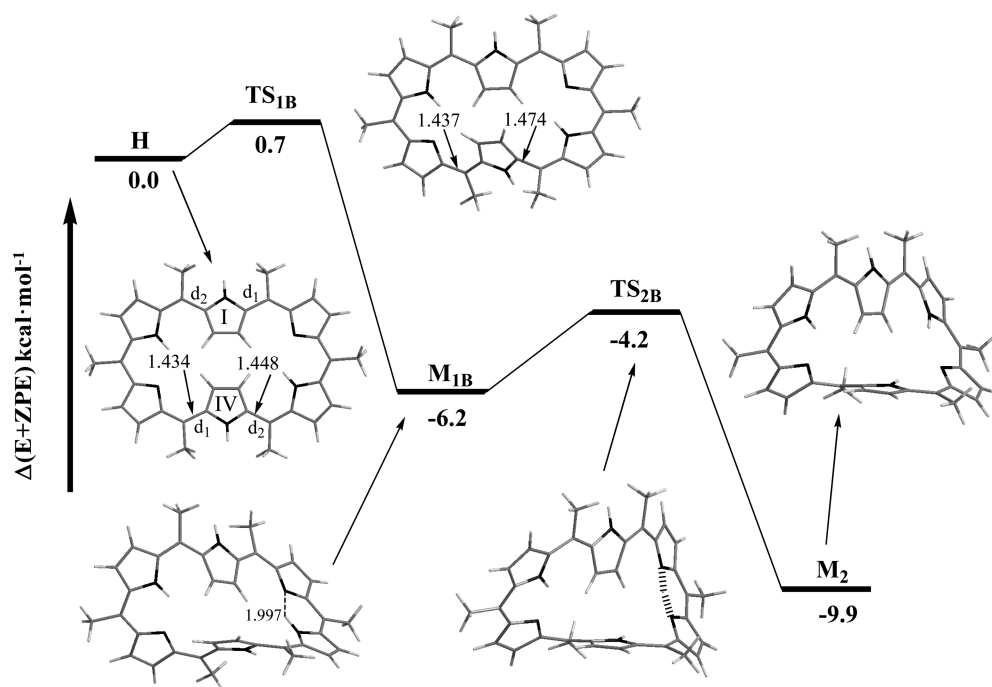
enthalpies, and free energies of these mechanisms for the eight meso-substituents considered in this work are contained in Tables 1 and 2.

The mechanism A (B) starts with the transition state TS<sub>1A</sub> (TS<sub>1B</sub>), which mainly implies a rotation around the  $d_1$  ( $d_2$ ) bond of the pyrrole unit I or IV (see Scheme 1). After this transition state, a Möbius structure M<sub>1A</sub> (M<sub>1B</sub>) is formed, which

shows a short hydrogen bond distance between the N and N-H of the pyrrolic rings II and III, respectively. Then, an easy proton transfer between both nitrogen atoms through TS<sub>2A</sub> (TS<sub>2B</sub>) is possible. In both mechanisms, the proton-transfer process leads to the same Möbius tautomer, M<sub>2</sub>, which is more stable than the M<sub>1A</sub> and M<sub>1B</sub> conformations.



**Figure 1.** Schematic potential energy surface evaluated at the M05-2X/6-311G(d,p) level for the interconversion between Hückel and Möbius structures for the F substituent via mechanism B.



**Figure 2.** Schematic potential energy surface evaluated at the M05-2X/6-311G(d,p) level for the interconversion between Hückel and Möbius structures for the CH<sub>3</sub> substituent via mechanism B.

In Tables 1 and 2, we can see that mechanisms A and B show a similar potential energy surface, although relevant differences can be found. For instance, the energy barrier associated with the rotational process of mechanism B (TS<sub>1B</sub>) is smaller (around 3 kcal·mol<sup>-1</sup>) than in mechanism A (TS<sub>1A</sub>), with the only exception being the NH<sub>2</sub> meso-substituent, which shows an energy barrier in TS<sub>1A</sub> 0.9 kcal·mol<sup>-1</sup> smaller than in TS<sub>1B</sub>. In addition, M<sub>1A</sub> and M<sub>1B</sub> structures have similar stabilities with respect to the Hückel conformation (H<sub>1</sub>), although M<sub>1A</sub> is

generally a bit more stable than M<sub>1B</sub> (around 1–2 kcal·mol<sup>-1</sup>). In contrast to the rotational process, the mechanism B has higher energy barriers for the proton-transfer process (the energy differences of the TS<sub>2A</sub> and TS<sub>2B</sub> with respect to M<sub>1A</sub> and M<sub>1B</sub>, respectively) than the mechanism A (by around 1–2 kcal·mol<sup>-1</sup>). All these aspects will be analyzed in more detail in the incoming paragraphs.

Major differences are obtained when the comparison is based on the results of the different meso-substituents, pointing to



**Table 3.** Selected Bond Distances (Å) and Bond Orders, NICS (ppm), HOMA, and Charge of the Ring (electrons) Values for All the Hückel ( $H_1$ ) and Möbius ( $M_2$ ) Structures Studied in This Work

subst	species	$d_1$	$d_2$	BO( $d_1$ )	BO( $d_2$ )	NICS	HOMA <sup>a</sup>	$Q_{RING}$ <sup>b)</sup>
H	$H_1$	1.424	1.435	1.244	1.217	10.33	0.62	-5.16
	$M_2$	1.420	1.424	1.262	1.250	-9.61	0.71	-5.23
CN	$H_1$	1.440	1.445	1.160	1.148	7.88	0.61	-4.02
	$M_2$	1.432	1.435	1.177	1.174	-8.48	0.68	-4.07
F	$H_1$	1.420	1.430	1.204	1.178	9.52	0.65	-1.89
	$M_2$	1.421	1.423	1.201	1.196	-9.55	0.75	-1.92
CH <sub>3</sub>	$H_1$	1.434	1.448	1.203	1.165	7.52	0.56	-4.06
	$M_2$	1.428	1.443	1.212	1.195	-8.57	0.70	-4.15
PhF <sub>2</sub>	$H_1$	1.435	1.448	1.111	1.068	7.19	0.57	-3.79
	$M_2$	1.427	1.433	1.126	1.119	-7.92	0.63	-3.86
PhF <sub>5</sub>	$H_1$	1.438	1.455	1.102	1.053	4.34	0.53	-3.78
	$M_2$	1.428	1.434	1.124	1.116	-7.75	0.69	-3.82
OH	$H_1$	1.354	1.365	1.497	1.459	6.63	0.69	-2.68
	$M_2$	1.359	1.361	1.483	1.469	-4.76	0.68	-2.71
NH <sub>2</sub>	$H_1$	1.368	1.381	1.448	1.414	3.45	0.73	-3.57
	$M_2$	1.367	1.367	1.476	1.456	-3.85	0.65	-3.57

<sup>a</sup>To see the paths used to calculate the HOMA values of the  $H_1$  and  $M_2$  structures, see Figure S3 (Supporting Information). <sup>b</sup>Only the heavy atoms of the porphyrin ring have been considered, evaluated using NBO charges at the M05-2X/6-311G(d,p) level.

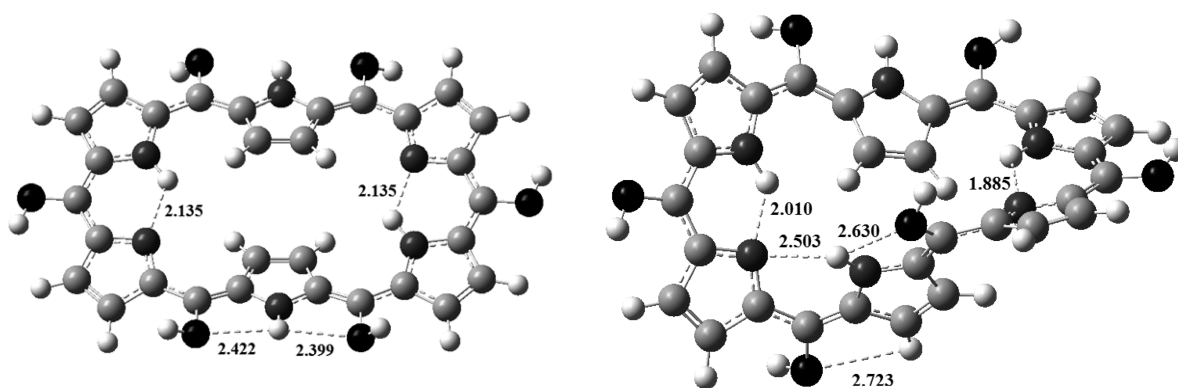
their crucial role in the thermochemistry and kinetics of these Hückel-to-Möbius topological switches. For instance, it is possible to move from a switch with an endothermic (6.8 kcal·mol<sup>-1</sup>) interconversion process with a considerable energy barrier (14.6 kcal·mol<sup>-1</sup>) to a switch with an exothermic (-9.9 kcal·mol<sup>-1</sup>) process and almost barrierless (0.7 kcal·mol<sup>-1</sup>) only by replacing the fluorine meso-substituent with a methyl substituent (see Tables 1 and 2 and Figures 1 and 2).

The energy barriers of the rotation process broadly range from 16.5 (TS<sub>1A</sub> for OH meso-substituent) to 0.7 (TS<sub>1B</sub> for CH<sub>3</sub> meso-substituent) kcal·mol<sup>-1</sup>. In our previous work, we proposed the lengths of  $d_1$  and  $d_2$  bond distances as estimators of the floppiness of the structure (ring strain), which can be directly linked to the energy barrier of the rotational process. To check further this hypothesis, we have also considered bond orders as descriptors of ring strain. Table 3 contains the  $d_1$  and  $d_2$  bond distances and their bond orders for all the  $H_1$  and  $M_2$  structures studied in this work. The bond distances and bond orders vary from 1.354 Å and 1.497 ( $d_1$  of the  $H_1$  structure for the OH meso-substituent) to 1.455 Å and 1.053 ( $d_2$  of the  $H_1$  structure for the PhF<sub>5</sub> meso-substituent), respectively. In Table 3, one can also see that long (short)  $d_1$  and  $d_2$  bond distances are associated with bond order values close to 1.1 (1.5), indicating a predominant single-bond-order character (conjugated bond order character). It should be expected that the more conjugated the character of the rotating bond, the more energetically expensive the rotation is. Interestingly, across all models,  $H_1$  structures show longer (smaller)  $d_2$  bond distances (bond orders) than  $d_1$ . This is consistent with the higher energy barriers observed for the rotational process in mechanism A (TS<sub>1A</sub> > TS<sub>1B</sub>), with the exception of the NH<sub>2</sub> meso-substituent, *vide supra*. Overall, an acceptable correlation is achieved between the  $d_1$  and  $d_2$  bond distances and the TS<sub>1A</sub> and TS<sub>1B</sub> energy barriers (see Figure S2, Supporting Information). All these results support the idea that a qualitative estimation of the ring strain can be obtained from the  $d_1$  and  $d_2$  bond distances. It is important to remark that the analysis of the ring strain only considering these two distances is a useful, but rough, approximation, as TS<sub>1A</sub> and TS<sub>1B</sub> structures not only involve the rotation of the central pyrrole

rings (labeled as I and IV, see Scheme 1) but also a reorganization of the other pyrrole rings.

The TS<sub>1A</sub> and TS<sub>1B</sub> conformations for the hydrogen meso-substituent lie 10.3 and 6.9 kcal·mol<sup>-1</sup>, respectively, above the Hückel structure. In the case of the CN (PhF<sub>2</sub>) meso-substituent there is a slight reduction of 2.1 and 1.2 (2.6 and 2.1) kcal·mol<sup>-1</sup> for the rotational energy barriers of the mechanisms A and B, respectively, with respect to the hydrogen meso-substituent. This reduction of the energy barrier becomes more important for the CH<sub>3</sub> (PhF<sub>5</sub>) meso-substituent, with TS<sub>1A</sub> and TS<sub>1B</sub> structures lying 3.6 and 0.7 (4.8 and 3.4) kcal·mol<sup>-1</sup>, respectively, above  $H_1$ . The  $d_1$  and  $d_2$  bond distances for the Hückel structure of the CN (PhF<sub>2</sub>) meso-substituent are elongated 0.016 and 0.010 (0.011 and 0.013) Å, respectively, with respect to the Hückel conformation of the H meso-substituent. The replacement of the hydrogen by the cyano and 2,6-fluorophenyl groups as a meso-substituent entails an increase of the steric effect and an enlargement of the  $d_1$  and  $d_2$  bond distances of the Hückel structure, i.e., a decrease of the overlap between the  $\pi$  orbitals and a reduction of the rotational energy barrier with respect to the H meso-substituent. The CH<sub>3</sub> and PhF<sub>5</sub> groups show similar increases of the  $d_1$  and  $d_2$  distances (ranging between 0.010 and 0.020 Å) to the CN and PhF<sub>2</sub> meso-substituents, although the former groups show larger steric effects. This fact can be understood by comparing their corresponding Hückel geometrical conformations; see Figure S1 (Supporting Information). The large size of the methyl and pentafluorophenyl groups provokes distortions of the planarity of the porphyrin rings, and their Hückel conformations become closer to the geometry of the rotational transition states (TS<sub>1A</sub> and TS<sub>1B</sub>), reducing their  $\pi$ -overlap and floppiness.<sup>34</sup> This fact can be noticed in the  $\angle C_1C_2C_3C_4$  dihedral angle (see Scheme 1) of the Hückel structure; the CH<sub>3</sub> and PhF<sub>5</sub> meso-substituents show  $\angle C_1C_2C_3C_4$  values of -24.2° and -36.5°, respectively, which represent an important distortions of the planarity with respect to the H meso-substituent, -17.8°.

On the other hand, the fluorine, hydroxyl, and amino groups increase (reduce) the rotational energy barriers ( $d_1$  and  $d_2$  bond distances) of the mechanisms A and B with respect to the



**Figure 3.**  $H_1$  (left) and  $M_2$  (right) conformations for the hydroxyl meso-substituent. Bond distances in angstroms and bond angles in degrees.

hydrogen meso-substituent. Their  $TS_{1A}$  and  $TS_{1B}$  conformations lie in a range between 9.3 ( $TS_{1B}$  for the F meso-substituent) and 16.5 ( $TS_{1A}$  for the OH meso-substituent) kcal·mol<sup>-1</sup> above the Hückel structures. The fluorine group provokes a small shortening of the  $d_1$  and  $d_2$  distances of the  $H_1$  conformation and a small increase of the rotational energy barriers (around 2 kcal·mol<sup>-1</sup>) with respect to the hydrogen model. With hydroxyl and amino meso-substituents, the rotational process of these [28]hexaphyrin rings becomes around 6 kcal·mol<sup>-1</sup> more expensive energetically than for the hydrogen substituent. These are the two systems where we found the highest energy barriers of interconversion. Two factors can explain this considerable enhancement of the energy barriers. First, their  $d_1$  and  $d_2$  bond distances in  $H_1$  are shortened to  $\sim 1.37$  Å, which means an average reduction of  $\sim 0.07$  Å with respect to the hydrogen model. Interestingly, these bond distances also show a relevant increase in the bond order ( $\sim 1.45$ ), implying a considerable increase in the  $\pi$ -overlap and rotational energy barrier. Second, the oxygen and nitrogen atoms of the hydroxyl and amino meso-substituents, respectively, can form intramolecular hydrogen bonds with the H–N and H–C atoms of the neighboring pyrroles (see Figure 3 and Figure S1, Supporting Information).<sup>35</sup> Then, a second argument of the increment of the energy barrier is that the rotational process also disrupts one of these intramolecular hydrogen bonds formed between the hydroxyl or amino group and the H–N atom of the pyrrole unit I or IV. It should be noted that both factors are inter-related as a reduction of  $d_1$  and  $d_2$  distances improves the geometry of the hydrogen bonds between the meso-group and the NH group of the pyrrole unit. This illustrates a relevant feature of the hexaphyrin switch: mutual interactions between meso-substituents and the central pyrrole units I and IV are very important as have a direct impact on the critical  $d_1$  and  $d_2$  bond distances as well as on the area subjected to a larger deformation along the Hückel–Möbius transition. We show later how this line of thought can be used as a design strategy for hexaphyrin switches.

The  $M_{1A}$  and  $M_{1B}$  structures lie in a large range of stabilities between  $-7.9$  ( $M_{1A}$  for CH<sub>3</sub>) and  $8.5$  ( $M_{1B}$  for F) kcal·mol<sup>-1</sup> with respect to the Hückel conformation, depending on the meso-substituent. It is important to remark that both structures have three intramolecular hydrogen bonds (N···H–N) inside the porphyrin ring. Their distances in the  $M_{1A}$  conformation are a bit shorter than in  $M_{1B}$ , which is consistent with the slightly higher stability of  $M_{1A}$  with respect to  $M_{1B}$  (around 1–2 kcal·mol<sup>-1</sup>). Interestingly, in contrast to the broad range of rotational energy barriers (around 15 kcal·mol<sup>-1</sup>), the energy

barriers of the proton-transfer process from  $M_1$  conformations to the more stable Möbius tautomer,  $M_2$  (i.e.,  $TS_{2A}$  and  $TS_{2B}$  with respect to  $M_{1A}$  and  $M_{1B}$ , respectively), vary within a narrower range that goes from 1.4 ( $TS_{2A}$  of the CH<sub>3</sub> meso-substituent) to 6 ( $TS_{2B}$  of the F meso-substituent) kcal·mol<sup>-1</sup>. We also note that the proton-transfer process tends to be energetically more expensive for those  $M_{1A}$  and  $M_{1B}$  conformations with longer hydrogen-bond distances between the N and N–H of the pyrrole units labeled as II and III, respectively. For instance, the hydrogen-bond distances of the  $M_{1A}$  and  $M_{1B}$  structures for the CH<sub>3</sub> and F meso-substituents are 1.89 and 2.05 Å, respectively, and this entails a difference of 4.6 kcal·mol<sup>-1</sup> in the proton-transfer barrier. Last, but not least, the proton-transfer process leads to a more stable Möbius tautomer,  $M_2$ , which also lies in a broad range of stabilities, between  $-9.9$  (CH<sub>3</sub>) and 6.8 (F) kcal·mol<sup>-1</sup> with respect to the Hückel conformation, depending on the substituent.

In the hexaphyrin model with the hydroxyl meso-substituent considered in this work, it is possible to consider that one and two hydroxyl groups can show a tautomerization process between the enol form ( $-C_{\text{meso}}-\text{OH}-\text{C}-\text{N}-$ ) and the keto ( $-C_{\text{meso}}=\text{O}-\text{C}-\text{NH}-$ ) form, generating two different oxophlorins or oxyporphyrins,<sup>36</sup> namely OH\_CO and OH\_2CO models, respectively. The conformational switch between Hückel and Möbius topologies of these two oxyporphyrins has also been studied (for more details, see the results reported in the Table S2 and Figure S4 of the Supporting Information). The replacement of one/two enols by one/two keto groups results in an important stabilization of the Hückel structures (around 10 and 20 kcal·mol<sup>-1</sup> in the first and second tautomerization process, respectively). Moreover, it changes the rearrangement of single and double bonds within the imidazole, e.g., the  $d_1$  and  $d_2$  bond distances of the Hückel structures for the OH\_CO and OH\_2CO models are elongated around 0.08 Å with respect to the OH model, and consequently, their rotational barriers show a significant reduction around 4–5.5 kcal·mol<sup>-1</sup>.

**Factors Affecting the Relative Stability between Hückel and Möbius Conformations.** To understand the origin of these important differences in the relative stability between Hückel and Möbius structures among the systems considered in this work, we have studied their aromaticity and their porphyrins ring charges, and in addition, we have also made an energy decomposition analysis (EDA). Table 3 contains two different aromaticity descriptors (the NICS at the geometrical ring center of the 36 heavy atoms forming the Hückel and Möbius rings and the HOMA indices; see Figure

S2 of the Supporting Information) for all the  $H_1$  and  $M_2$  structures considered in this work. The  $M_2$  ( $H_1$ ) conformations show negative (positive) NICS values and larger (smaller) HOMA values than  $H_1$  ( $M_2$ ). The results obtained for both descriptors are consistent with the idea that in  $4n$   $\pi$ -electron conjugated systems, like the hexaphyrins studied here, the Möbius species is aromatic, in contrast to the Hückel conformation, which is antiaromatic. However, a clear relationship between relative stabilities and aromaticity is not observed. For instance, the  $H_1$  and  $M_2$  structures with the methyl group, where  $M_2$  lies 9.9 kcal·mol<sup>-1</sup> below  $H_1$ , have more similar NICS values than the  $H_1$  and  $M_2$  conformations with the hydrogen substituent, where  $M_2$  lies 2.0 kcal·mol<sup>-1</sup> above  $H_1$ . Although Möbius aromaticity must be a source of stability with respect to the antiaromatic Hückel species, these results indicate that it plays a smaller role in the relative stability of both structures than other effects, e.g., ring strain, steric effect, and hydrogen bonds. Moreover, one can see in Table 3 that the Hückel and Möbius structures show very similar porphyrin ring charges ( $M_2$  only contains around 0.05 more electrons than  $H_1$ ). Independently of the nature of the group, all the meso-substituents withdraw electrons from the porphyrins ring, considering the hydrogen group as reference, and in particular, this inductive effect is more important for the meso-substituents with highly electronegative atoms (O, N, and F). We note that changes in the porphyrin ring charge do not correlate with changes in the thermochemistry and/or kinetics of these topological switches.

The energy decomposition analysis<sup>27</sup> allows us to partition the interaction energy between the atomic fragments building the molecule into three different components: (1) Pauli repulsion ( $E_{\text{Pauli}}$ , a positive energy value), which is the repulsive interaction between atomic fragments due to impossibility that two electrons of the same spin occupy the same space, i.e., steric effect; (2) electrostatic energy ( $E_{\text{elstat}}$ , a negative energy value) between the frozen electron densities of the fragments; (3) orbital interaction energy ( $E_{\text{oi}}$ , a negative energy value), i.e., charge-transfer between the occupied orbitals of one fragment and the unoccupied ones of another fragment. The sum of these terms is the interaction energy,  $E_{\text{int}}$ . Accordingly, we have decomposed the relative stability between Hückel ( $H_1$ ) and Möbius ( $M_2$ ) structures of each meso-substituted hexaphyrin in these three different components. Table 4 summarizes the change in each EDA component and the relative stabilities between the  $H_1$  and  $M_2$  structures computed at the

**Table 4. Energy Decomposition Analysis of the Hückel ( $H_1$ ) and Möbius ( $M_2$ ) Structures Studied in This Work<sup>a</sup>**

subst	$\Delta E_{\text{Pauli}}$	$\Delta E_{\text{elstat}}$	$\Delta E_{\text{oi}}$	$\Delta E_{\text{int}}$	$\Delta E^b$
H	-27.6	-23.0	56.7	6.1	5.6
CN	8.2	-13.1	7.5	2.6	3.1
F	-4.7	-26.1	39.0	8.1	7.0
CH <sub>3</sub>	-34.3	-21.5	50.0	-5.8	-6.2
PhF <sub>2</sub>	1.4	-7.9	3.9	-2.6	-1.5
PhF <sub>3</sub>	21.5	-7.1	-22.4	-8.0	-6.9
OH	-104.9	4.3	106.1	5.5	6.5
NH <sub>2</sub>	-131.6	17.7	113.0	-0.9	-1.2

<sup>a</sup>Reported values for each energy component correspond to the energy difference between  $M_2$  and  $H_1$  structures for each system and are given in kcal·mol<sup>-1</sup>. <sup>b</sup>Relative energies computed at the BH&HLYP/TZP//M05-2X/6-311G(d,p) level using the ADF program package.

BH&HLYP/TZP//M05-2X/6-311G(d,p) level using the ADF program package.<sup>37</sup>

With the exception of the PhF<sub>5</sub> model, for all hexaphyrins the energy differences between the relative stabilities evaluated using the BH&HLYP/TZP and M05-2X/6-311G(d,p) methodologies are less than 3 kcal·mol<sup>-1</sup> (the PhF<sub>5</sub> meso-substituent is a peculiar case and it will be discussed at the end of this section). In addition, the energy differences between the  $\Delta E_{\text{int}}$  and  $\Delta E$  values calculated at BH&HLYP/TZP level are also less than 3.5 kcal·mol<sup>-1</sup>, indicating that the energy decomposition analysis can be used to rationalize the important differences in the relative stabilities using different meso-substituents. In general, the  $H_1 \rightarrow M_2$  transition entails a decrease of the steric ( $\Delta E_{\text{Pauli}} < 0$ , except for the CN and PhF<sub>2</sub> groups) and electrostatic ( $\Delta E_{\text{elstat}} < 0$ , except for the OH and NH<sub>2</sub> groups) effects and an increase in the orbital interaction energy ( $\Delta E_{\text{oi}} > 0$ ).

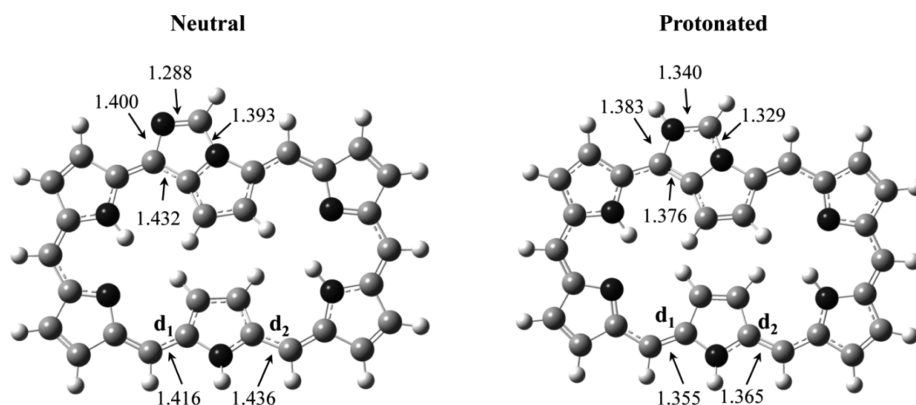
In relation to the steric effect, one can initially consider that the higher stability of Möbius species with respect to the Hückel one is due to the fact that the meso-substituents between pyrroles III and IV and the pyrroles IV and V are placed in opposite sides of the Möbius strip (see Scheme 1), whereas in the Hückel conformation these two meso-substituents are in the same side and closer in space to the central pyrrole IV, thus leading to a higher steric effect. However, from the results of Table 4 we can see that this point of view is simplistic and the situation is more complex because the rotational process implies the rearrangement of several distances along the porphyrin ring.

It is worth noting that the terms of the dipole moment for the  $H_1$  conformations are null or negligible (in contrast to  $M_2$ ) and that the  $H_1$  and  $M_2$  structures present two and three intramolecular hydrogen bonds, respectively. These two factors explain that the Möbius conformations present lower (more stable) electrostatic energy than the Hückel ones. The newly formed hydrogen bond in the Möbius structure arises from the rotating pyrrole ring, which now properly orients the NH bond to the inner ring and donates a hydrogen bond to the nonprotonated N site of the adjoining pyrrole ring (see Figure S1, Supporting Information). This tendency of the electrostatic energy is opposite in the cases of the OH and NH<sub>2</sub> groups as two hydrogen bonds are strongly weakened in the  $M_2$  structure (see Figure 3 and Supporting Information). In particular, one C–HO···H–N (C–H<sub>2</sub>N···H–N) hydrogen bond has an important elongation (around 0.3 Å) and the other is broken as a result of the rotation.

In the orbital interaction energy values, we can find another indication that aromaticity plays a small role in the thermochemistry of these topological switches. The  $E_{\text{oi}}$  contains several stabilization effects, among them the aromaticity,<sup>38</sup> and the Hückel conformations (in exception of the PhF<sub>5</sub> meso-substituent) show lower (more stable) orbital interaction energy values than the Möbius structures,  $\Delta E_{\text{oi}} > 0$ . This fact also points out that the remaining charge-transfers between the occupied orbitals of one fragment and the unoccupied ones of another fragment, e.g., ring strain, are more important than the aromaticity.

The  $\Delta E_{\text{int}}$  is the only EDA term that correlates with the relative stabilities between Hückel and Möbius structures, indicating that  $\Delta E$  can only be analyzed considering the balance between the three EDA components ( $\Delta E_{\text{Pauli}}$ ,  $\Delta E_{\text{elstat}}$  and  $\Delta E_{\text{oi}}$ ). For the H and F models, the decrease in orbital interaction for the Möbius species is not compensated by the





**Figure 4.** Representation of the Hückel conformation of a [28]hexaphyrin(1.1.1.1.1.1) with a fused imidazole ring at one meso-position. Two protonation states of the imidazole group are shown. The rotating bonds of the Hückel–Möbius transition described in the text are labeled as  $d_1$  and  $d_2$ .

**Table 5. Relative Energies, Energies plus Zero Point Energies, Enthalpies, and Free Energies for the Hückel → Möbius Switch with a Imidazolic Meso-Substituent via the Two Mechanisms (A and B) Evaluated at the M05-2X/6-311G(d,p) Level<sup>a</sup>**

subst	species	mechanism A				mechanism B				
		$\Delta E$	$\Delta(E+ZPE)$	$\Delta H$	$\Delta G$	$\Delta E$	$\Delta(E+ZPE)$	$\Delta H$	$\Delta G$	
Neutral	H <sub>1</sub>	0.00	0.00	0.00	0.00	H <sub>1</sub>	0.00	0.00	0.00	0.00
	TS <sub>1A</sub>	10.45	10.39	9.86	11.45	TS <sub>1B</sub>	8.40	8.25	7.67	9.27
	M <sub>1A</sub>	-2.67	-2.39	-2.53	-2.24	M <sub>1B</sub>	-0.11	0.17	0.15	0.03
	TS <sub>2A</sub>	4.91	2.30	1.84	3.09	TS <sub>2B</sub>	9.60	6.64	6.37	6.90
	M <sub>2A</sub>	-3.32	-2.95	-3.17	-2.56	M <sub>2B</sub>	-0.67	-0.45	-0.51	-0.88
Protonated	H <sub>1</sub>	0.00	0.00	0.00	0.00	H <sub>1</sub>	0.00	0.00	0.00	0.00
	TS <sub>1A</sub>	23.69	22.72	22.31	23.65	TS <sub>1B</sub>	18.39	17.15	16.73	17.86
	M <sub>1A</sub>	5.05	4.52	4.44	4.68	M <sub>1B</sub>	6.95	6.37	6.41	6.08
	TS <sub>2A</sub>	12.11	8.66	8.34	9.19	TS <sub>2B</sub>	16.11	12.52	12.27	12.82
	M <sub>2A</sub>	4.56	4.09	3.99	4.32	M <sub>2B</sub>	5.93	5.49	5.47	5.19

<sup>a</sup>Both neutral and protonated states of the imidazolic group have been considered. All quantities are in kcal·mol<sup>-1</sup> and  $T = 298$  K.

lower steric effect and electrostatic energy, being more stable the Hückel structure. On the other hand, the CH<sub>3</sub> model exhibits stronger steric effects, due to the bulkier methyl groups, favoring the Möbius conformation. The CN and PhF<sub>2</sub> meso-substituents present small and positive  $\Delta E_{\text{Pauli}}$  and  $\Delta E_{\text{oi}}$  values and negative  $\Delta E_{\text{elstat}}$ , but the different balance of their components leads to opposite H → M relative interaction energies (2.6 and -2.6 kcal·mol<sup>-1</sup>, respectively). In the OH and NH<sub>2</sub> groups, large variations of  $E_{\text{Pauli}}$  and  $E_{\text{oi}}$ , which cancel each other, in combination with positive  $\Delta E_{\text{elstat}}$  values make the H<sub>1</sub> and M<sub>2</sub> for the OH and NH<sub>2</sub> meso-substituents, respectively, more stable than their corresponding M<sub>2</sub> and H<sub>1</sub> conformations. The balance between  $\Delta E_{\text{Pauli}}$ ,  $\Delta E_{\text{elstat}}$ , and  $\Delta E_{\text{oi}}$  terms is a very subtle problem and similar groups with similar reactivity trends can exhibit different relative stabilities. The PhF<sub>5</sub> is the only meso-substituent that shows a negative  $\Delta E_{\text{oi}}$  (-22.4 kcal·mol<sup>-1</sup>) and a positive and large  $\Delta E_{\text{Pauli}}$  (21.5 kcal·mol<sup>-1</sup>) value, and as both components cancel each other, the stabilization of  $\Delta E_{\text{elstat}}$  becomes closely similar to the relative interaction energy. It is important to remark that the PhF<sub>5</sub> group presents the largest energy difference (around 6 kcal·mol<sup>-1</sup>) between the relative stabilities evaluated with the BH&HLYP/TZP and M05-2X/6-311G(d,p) methodologies; i.e., the EDA results obtained for this case have to be considered with some skepticism.

**Exploiting Meso-Substituent Effects for Designing Novel Hückel–Möbius Switches.** In the present investigation we have described a variety of effects of the meso-

substituent in the thermodynamics and kinetics of the conformational switch. Here, we anticipate that such effects should inspire the design of novel Hückel–Möbius topological switches with desired kinetic and thermodynamic properties. In particular, it would be of great interest the design of new Hückel–Möbius switches that change their thermodynamic equilibrium and the kinetics of its interconversion as a response to changes in external conditions such as pH or temperature.

To illustrate how the meso-effects pointed out above can be exploited for designing a switch responsive to the environment, it is instructive to consider the model of a Hückel–Möbius switch shown in Figure 4. In this case, one meso-substituent of the hexaphyrin is cyclic (the remaining meso-substituents are hydrogen atoms) and builds an imidazole group fused to the central pyrrole ring. The interesting feature of such group is that the nonpyrrolic nitrogen is a basic site and thus can be protonated. It is worth pointing out that this system is not symmetric, and thus, mechanisms A and B lead to non-equivalent M<sub>2</sub> conformers, herein referred as M<sub>2A</sub> and M<sub>2B</sub>, respectively. Figure 4 illustrates how the protonation of this nitrogen leads to a rearrangement of single and double bonds within the imidazole ring that, in turn, is propagated to the rest of the hexaphyrin. It is particularly interesting that the extent to which the protonation of the meso-group shortens the rotating C–C bonds of the two most accessible H → M transitions ( $d_1$  and  $d_2$  in Figure 4); i.e.,  $d_1$  and  $d_2$  decrease from 1.416 and 1.436 to 1.355 and 1.365 Å, respectively, upon protonation. According to our previous observations, changes in these



specific bond distances have important effects on the kinetics of the  $M \rightarrow H$  interconversion (shorter bond distances tend to raise the energy barrier for the  $H \rightarrow M$  transition). Table 5 shows that upon protonation the transition state increases 12.3 and 8.9 kcal·mol<sup>-1</sup> for mechanisms A and B, respectively. Moreover, while the Möbius species  $M_{2A}$  and  $M_{2B}$  are more favored in the neutral state by -3.0 and -0.5 kcal·mol<sup>-1</sup>, respectively, the protonation inverts the relative stability between Möbius and Hückel species, with the Hückel species being more stable by 4.1 and 5.5 kcal·mol<sup>-1</sup> with respect to the two possible Möbius species ( $M_{2A}$  and  $M_{2B}$ ). In principle, this suggests that a decrease in pH would favor the Hückel species, given its higher thermodynamic stability and higher energy barrier for the  $H \rightarrow M$  transition. Conversely, increases in pH would thermodynamically favor the Möbius species and also at a higher rate of interconversion. Furthermore, if pH changes the energy barrier of the  $H-M$  transition, the effect of temperature on the switch interconversion rate will change accordingly. Therefore, pH and temperature can provide thermodynamic and kinetic control of the topological switch. It is pertinent to note that other pyrrole nitrogen sites may compete for protonation and also that the incorporation of solvent effects would affect the relative stability of the different species here described. However, it should be clear to the readers that this system is just a model, which not necessarily can be reproduced from an experimental point of view and only aims to illustrate the variety of possibilities that meso-substituents offer for designing novel hexaphyrin-based switches responsive to external conditions that are easily controllable, such as pH and temperature. Therefore, we consider that further research should be done in this issue to clarify the effect of external conditions.

## ■ CONCLUSIONS AND FUTURE WORK

In the present work, we have performed a theoretical study aiming at the evaluation of the effect of the meso-substituent in the conformational switch between Hückel planar and Möbius twisted topologies for [28]hexaphyrins. Eight different meso-substituents (hydrogen, cyano, fluorine, methyl, 2,6-fluorophenyl, pentafluorophenyl, hydroxyl, and amino) with different steric effects and electron-withdrawing and -releasing characters have been considered, and calculations were performed at the M05-2X/6-311G(d,p) level. The obtained results highlight the following conclusions:

(a) The nature of the meso-substituent is important for determining the relative stability of the Hückel–Möbius conformers and also for controlling the barrier height of the interconversion between them. Thus, for instance, the replacement of a fluorine meso-substituent by a methyl group results in a change from an endothermic (6.8 kcal·mol<sup>-1</sup>) interconversion process with a high energy barrier (14.6 kcal·mol<sup>-1</sup>) into an exothermic (-9.9 kcal·mol<sup>-1</sup>) interconversion process, which is almost barrierless (0.7 kcal·mol<sup>-1</sup>). The results of this investigation allow us to conclude that the nature of the meso-substituent plays a critical role on the thermochemistry and kinetics of the Hückel-to-Möbius interconversion and can be a tool for controlling these topological switches.

(b) In agreement with our previous results,<sup>12</sup> we have confirmed with a large set of meso-substituents that the  $d_1$  and  $d_2$  bond distances can be regarded as good estimators of the floppiness of the structure (ring strain), which can be directly linked to the energy barriers of the rotational process. However,

it is worth noting that other factors can also be very relevant such as hydrogen bond interactions between meso-substituents and the central pyrrole units I and IV.

(c) Aromaticity indices point to the more aromatic character of the Möbius species, but we do not find a correlation between aromaticity and stability. Importantly, the interplay between other factors, e.g., ring strain, steric effect, and hydrogen bonds, plays a more important role than aromaticity in determining the relative stability between Hückel and Möbius conformations.

(d) The results obtained with the partition of the interaction energy into Pauli repulsion, electrostatic energy, and orbital interaction energy show that the prediction of the relative stability between Hückel and Möbius structures is a complex and subtle problem (similar groups with similar reactivity trends can exhibit different stabilities). Only the sum of these three terms correlates with the relative stabilities between both conformations. Nevertheless, the energy decomposition analysis provides a qualitative understanding of how different meso-substituents affect the balance of these three factors and thus modulate the relative stability between Hückel and Möbius species.

All these results are very useful for rationalizing past experimental results and designing future experiments, e.g., controlling the thermochemistry and kinetics of these topological switches. As an illustrative example, we have proposed a “toy model” of a hexaphyrin switch responsive to the environment. In this model, one meso-substituent is an imidazole group that is fused to the central pyrrole ring. Interestingly, changes in the protonation state of the meso-substituent provoke a rearrangement of single and double bonds in the imidazole ring that is propagated across the rest of the hexaphyrin, which results in important variations in the rotational energy barrier and the relative stability of the Hückel and Möbius conformations. A decrease in pH would favor the Hückel species, given its higher thermodynamic stability and higher energy barriers for the Hückel-to-Möbius transition. On the other hand, an increase in pH would favor the Möbius species.

This work paves the way to understanding crucial factors involved in the interconversion mechanism between Hückel and Möbius topologies for the [28]hexaphyrin. Additional work on the effect of combining different meso-substituents with different distributions of meso positions is in progress in our laboratory. As we will show elsewhere, the number and distribution of the meso-substituents have also a critical role in the thermochemistry and kinetics of these topological switches.

## ■ ASSOCIATED CONTENT

### 📄 Supporting Information

Hückel and Möbius conformations for the eight meso-substituents considered in this work; correlation between the rotational energy barriers ( $TS_{1A}$  and  $TS_{1B}$ ) and the  $d_1$  and  $d_2$  bond distances; paths used to calculate the HOMA values of the  $H$  and  $M_2$  structures; values of the energy decomposition analysis of the Hückel ( $H_1$ ) and Möbius ( $M_2$ ) structures studied in this work; relative energies, energies plus zero point energies, enthalpies, and free energies of the Hückel  $\rightarrow$  Möbius switch for two oxyporphyrins and their Hückel and Möbius conformations; Cartesian coordinates of all stationary points investigated in this work. This material is available free of charge via the Internet at <http://pubs.acs.org>.

## AUTHOR INFORMATION

### Corresponding Authors

\*E-mail: emarcos82@gmail.com. Phone: +34 934006111. Fax: +34 932045903.

\*E-mail: miqueltorrentsucarrat@gmail.com. Phone: +34 934006111. Fax: +34 932045903.

### Notes

The authors declare no competing financial interest.

## ACKNOWLEDGMENTS

This research has been supported by the Research Executive Agency (Grant Agreement No. PERG05-GA-2009-249310) and by the Generalitat de Catalunya (Grant No. 2009SGR01472). The calculations described in this work were carried out at the Centre de Supercomputació de Catalunya (CESCA). M.T-S. acknowledges the CSIC for the JAE-DOC contract, and E.M. acknowledges a contract under the PERG05-GA-2009-249310 grant. We are grateful to Pedro Salvador for his help with the fuzzy bond order calculations.

## REFERENCES

- (1) (a) Simkova, I.; Latos-Grażyński, L.; Stepień, M. *Angew. Chem., Int. Ed.* **2010**, *49*, 7665. Pacholska-Dudziak, E.; Szterenber, L.; Latos-Grażyński, L. *Chem.—Eur. J.* **2011**, *17*, 3500. (b) Pawlicki, M.; Latos-Grażyński, L. *Angew. Chem., Int. Ed.* **2012**, *51*, 11205. (c) Tokuji, S.; Yorimitsu, H.; Osuka, A. *Angew. Chem., Int. Ed.* **2012**, *51*, 12357. (d) Chang, Y.; Chen, H.; Zhou, Z.; Zhang, Y.; Schuett, C.; Herges, R.; Shen, Z. *Angew. Chem., Int. Ed.* **2012**, *51*, 12801. (e) Okujima, T.; Kikkawa, T.; Nakano, H.; Kubota, H.; Fukugami, N.; Ono, N.; Yamada, H.; Uno, H. *Chem.—Eur. J.* **2012**, *18*, 12854. (f) Kon-no, M.; Mack, J.; Kobayashi, N.; Suenaga, M.; Yoza, K.; Shinmyozu, T. *Chem.—Eur. J.* **2012**, *18*, 13361. (g) Kamiya, H.; Kondo, T.; Sakida, T.; Yamaguchi, S.; Shinokubo, H. *Chem.—Eur. J.* **2012**, *18*, 16129. (h) Grocka, I.; Latos-Grażyński, L.; Stepień, M. *Angew. Chem., Int. Ed.* **2013**, *52*, 1044. (i) Gokulnath, S.; Nishimura, K.; Toganoh, M.; Mori, S.; Furuta, H. *Angew. Chem., Int. Ed.* **2013**, *52*, 6940. (j) Tokuji, S.; Awane, H.; Yorimitsu, H.; Osuka, A. *Chem.—Eur. J.* **2013**, *19*, 64. (k) Pacholska-Dudziak, E.; Szczepaniak, M.; Ksiazek, A.; Latos-Grażyński, L. *Angew. Chem., Int. Ed.* **2013**, *52*, 8898. (l) Blusch, L. K.; Hemberger, Y.; Proepper, K.; Ditttrich, B.; Witterauf, F.; John, M.; Bringmann, G.; Brueckner, C.; Meyer, F. *Chem.—Eur. J.* **2013**, *19*, 5868. (m) Karthik, G.; Sneha, M.; Raja, V. P.; Lim, J. M.; Kim, D.; Srinivasan, A.; Chandrasekar, T. K. *Chem.—Eur. J.* **2013**, *19*, 1886.
- (2) (a) Jux, N. *Angew. Chem., Int. Ed.* **2008**, *47*, 2543. (b) Stepień, M.; Sprutta, N.; Latos-Grażyński, L. *Angew. Chem., Int. Ed.* **2011**, *50*, 4288. (c) Saito, S.; Osuka, A. *Angew. Chem., Int. Ed.* **2011**, *50*, 4342.
- (3) (a) Shin, J. Y.; Kim, K. S.; Yoon, M. C.; Lim, J. M.; Yoon, Z. S.; Osuka, A.; Kim, D. *Chem. Soc. Rev.* **2010**, *39*, 2751. (b) Osuka, A.; Saito, S. *Chem. Commun.* **2011**, *47*, 4330. (c) Torrent-Sucarrat, M.; Anglada, J. M.; Luis, J. M. *J. Chem. Phys.* **2012**, *137*, 1184306.
- (4) (a) Stepień, M.; Latos-Grażyński, L.; Sprutta, N.; Chwalisz, P.; Szterenber, L. *Angew. Chem., Int. Ed.* **2007**, *46*, 7869. (b) Saito, S.; Shin, J. Y.; Lim, J. M.; Kim, K. S.; Kim, D.; Osuka, A. *Angew. Chem., Int. Ed.* **2008**, *47*, 9657. (c) Shin, J. Y.; Lim, J. M.; Yoon, Z. S.; Kim, K. S.; Yoon, M. C.; Hiroto, S.; Shinokubo, H.; Shimizu, S.; Osuka, A.; Kim, D. *J. Phys. Chem. B* **2009**, *113*, 5794. (d) Stepień, M.; Szyszko, B.; Latos-Grażyński, L. *J. Am. Chem. Soc.* **2010**, *132*, 3140. (e) Lim, J. M.; Shin, J. Y.; Tanaka, Y.; Saito, S.; Osuka, A.; Kim, D. *J. Am. Chem. Soc.* **2010**, *132*, 3105. (f) Yoon, M. C.; Shin, J. Y.; Lim, J. M.; Saito, S.; Yoneda, T.; Osuka, A.; Kim, D. *Chem.—Eur. J.* **2011**, *17*, 6707. (g) Cha, W. Y.; Lim, J. M.; Yoon, M. C.; Sung, Y. M.; Lee, B. S.; Katsumata, S.; Suzuki, M.; Mori, H.; Ikawa, Y.; Furuta, H.; Osuka, A.; Kim, D. *Chem.—Eur. J.* **2012**, *18*, 15838.
- (5) Sankar, J.; Mori, S.; Saito, S.; Rath, H.; Suzuki, M.; Inokuma, Y.; Shinokubo, H.; Kim, K. S.; Yoon, Z. S.; Shin, J. Y.; Lim, J. M.; Matsuzaki, Y.; Matsushita, O.; Muranaka, A.; Kobayashi, N.; Kim, D.; Osuka, A. *J. Am. Chem. Soc.* **2008**, *130*, 13568.
- (6) Kim, K. S.; Yoon, Z. S.; Ricks, A. B.; Shin, J. Y.; Mori, S.; Sankar, J.; Saito, S.; Jung, Y. M.; Wasielewski, M. R.; Osuka, A.; Kim, D. *J. Phys. Chem. A* **2009**, *113*, 4498.
- (7) Yoon, M. C.; Kim, P.; Yoo, H.; Shimizu, S.; Koide, T.; Tokuji, S.; Saito, S.; Osuka, A.; Kim, D. *J. Phys. Chem. B* **2011**, *115*, 14928.
- (8) (a) Tanaka, Y.; Saito, S.; Mori, S.; Aratani, N.; Shinokubo, H.; Shibata, N.; Higuchi, Y.; Yoon, Z. S.; Kim, K. S.; Noh, S. B.; Park, J. K.; Kim, D.; Osuka, A. *Angew. Chem., Int. Ed.* **2008**, *47*, 681. (b) Park, J. K.; Yoon, Z. S.; Yoon, M. C.; Kim, K. S.; Mori, S.; Shin, J. Y.; Osuka, A.; Kim, D. *J. Am. Chem. Soc.* **2008**, *130*, 1824. (c) Tanaka, T.; Sugita, T.; Tokuji, S.; Saito, S.; Osuka, A. *Angew. Chem., Int. Ed.* **2010**, *49*, 6619. (d) Rath, H.; Tokuji, S.; Aratani, N.; Furukawa, K.; Lim, J. M.; Kim, D.; Shinokubo, H.; Osuka, A. *Angew. Chem., Int. Ed.* **2010**, *49*, 1489. (e) Inoue, M.; Yoneda, T.; Youfu, K.; Aratani, N.; Osuka, A. *Chem.—Eur. J.* **2011**, *17*, 9028. (f) Tanaka, T.; Osuka, A. *Chem.—Eur. J.* **2012**, *18*, 7036.
- (9) (a) Inoue, M.; Kim, K. S.; Suzuki, M.; Lim, J. M.; Shin, J. Y.; Kim, D.; Osuka, A. *Angew. Chem., Int. Ed.* **2009**, *48*, 6687. (b) Tokuji, S.; Shin, J. Y.; Kim, K. S.; Lim, J. M.; Youfu, K.; Saito, S.; Kim, D.; Osuka, A. *J. Am. Chem. Soc.* **2009**, *131*, 7240. (c) Higashino, T.; Inoue, M.; Osuka, A. *J. Org. Chem.* **2010**, *75*, 7958. (d) Higashino, T.; Lim, J. M.; Miura, T.; Saito, S.; Shin, J. Y.; Kim, D.; Osuka, A. *Angew. Chem., Int. Ed.* **2010**, *49*, 4950. (e) Higashino, T.; Lee, B. S.; Lim, J. M.; Kim, D.; Osuka, A. *Angew. Chem., Int. Ed.* **2012**, *51*, 13105.
- (10) (a) Mauksch, M.; Gogonea, V.; Jiao, H.; Schleyer, P. v. R. *Angew. Chem., Int. Ed.* **1998**, *37*, 2395. (b) Ajami, D.; Oeckler, O.; Simon, A.; Herges, R. *Nature* **2003**, *426*, 819. (c) Castro, C.; Chen, Z. F.; Wannere, C. S.; Jiao, H. J.; Karney, W. L.; Mauksch, M.; Puchta, R.; Hommes, N.; Schleyer, P. v. R. *J. Am. Chem. Soc.* **2005**, *127*, 2425. (d) Ajami, D.; Hess, K.; Kohler, F.; Nather, C.; Oeckler, O.; Simon, A.; Yamamoto, C.; Okamoto, Y.; Herges, R. *Chem.—Eur. J.* **2006**, *12*, 5434. (e) Warner, P. M. *J. Org. Chem.* **2006**, *71*, 9271. (f) Pemberton, R. P.; McShane, C. M.; Castro, C.; Karney, W. L. *J. Am. Chem. Soc.* **2006**, *128*, 16692. (g) Moll, J. F.; Pemberton, R. P.; Gutierrez, M. G.; Castro, C.; Karney, W. L. *J. Am. Chem. Soc.* **2007**, *129*, 274. (h) Bucher, G.; Grimme, S.; Huenerbein, R.; Auer, A. A.; Mucke, E.; Kohler, F.; Siegwirth, J.; Herges, R. *Angew. Chem., Int. Ed.* **2009**, *48*, 9971. (i) Mauksch, M.; Tsogoeva, S. B. *Angew. Chem., Int. Ed.* **2009**, *48*, 2959. (j) Mucke, E. K.; Kohler, F.; Herges, R. *Org. Lett.* **2010**, *12*, 1708.
- (11) Castro, C.; Karney, W. L.; Valencia, M. A.; Vu, C. M. H.; Pemberton, R. P. *J. Am. Chem. Soc.* **2005**, *127*, 9704.
- (12) Marcos, E.; Anglada, J. M.; Torrent-Sucarrat, M. *J. Phys. Chem. C* **2012**, *116*, 24358.
- (13) Alonso, M.; Geerlings, P.; de Proft, F. *Chem.—Eur. J.* **2012**, *18*, 10916.
- (14) Alonso, M.; Geerlings, P.; de Proft, F. *Chem.—Eur. J.* **2013**, *19*, 1617.
- (15) We note that the results of the H and PhF<sub>2</sub> substituents were already published in our previous article; see ref 12. They have been included in the present work for comparison purposes.
- (16) (a) King, R. A.; Crawford, T. D.; Stanton, J. F.; Schaefer, H. F. *J. Am. Chem. Soc.* **1999**, *121*, 10788. (b) Wannere, C. S.; Sattelmeyer, K. W.; Schaefer, H. F.; Schleyer, P. v. R. *Angew. Chem., Int. Ed.* **2004**, *43*, 4200. (c) Castro, C.; Karney, W. L.; Vu, C. M. H.; Burkhardt, S. E.; Valencia, M. A. *J. Org. Chem.* **2005**, *70*, 3602.
- (17) Zhao, Y.; Schultz, N. E.; Truhlar, D. G. *J. Chem. Theory Comput.* **2006**, *2*, 364.
- (18) (a) Hehre, W. J.; Ditchfield, R.; Pople, J. A. *J. Chem. Phys.* **1972**, *56*, 2257. (b) Hehre, W. J.; Radom, L.; Schleyer, P. v. R.; Pople, J. A. *Ab Initio Molecular Orbital Theory*; Wiley: New York, 1986.
- (19) (a) Krygowski, T. M.; Cyranski, M. *Tetrahedron* **1996**, *52*, 10255. (b) Krygowski, T. M.; Cyranski, M. K. *Chem. Rev.* **2001**, *101*, 1385.
- (20) (a) Schleyer, P. v. R.; Maerker, C.; Dransfeld, A.; Jiao, H. J.; Hommes, N. *J. Am. Chem. Soc.* **1996**, *118*, 6317. (b) Schleyer, P. v. R. *Chem. Rev.* **2001**, *101*, 1115. (c) Chen, Z. F.; Wannere, C. S.;

Corminboeuf, C.; Puchta, R.; Schleyer, P. v. R. *Chem. Rev.* **2005**, *105*, 3842.

(21) Frisch, M. J.; Trucks, G. W.; Schlegel, H. B.; Scuseria, G. E.; Robb, M. A.; Cheeseman, J. R.; Scalmani, G.; Barone, V.; Mennucci, B.; Petersson, G. A.; Nakatsuji, H.; Caricato, M.; Li, X.; Hratchian, H. P.; Izmaylov, A. F.; Bloino, J.; Zheng, G.; Sonnenberg, J. L.; Hada, M.; Ehara, M.; Toyota, K.; Fukuda, R.; Hasegawa, J.; Ishida, M.; Nakajima, T.; Honda, Y.; Kitao, O.; Nakai, H.; Vreven, T.; Montgomery, J. A., Jr.; Peralta, J. E.; Ogliaro, F.; Bearpark, M.; Heyd, J. J.; Brothers, E.; Kudin, K. N.; Staroverov, V. N.; Kobayashi, R.; Normand, J.; Raghavachari, K.; Rendell, A.; Burant, J. C.; Iyengar, S. S.; Tomasi, J.; Cossi, M.; Rega, N.; Millam, J. M.; Klene, M.; Knox, J. E.; Cross, J. B.; Bakken, V.; Adamo, C.; Jaramillo, J.; Gomperts, R.; Stratmann, R. E.; Yazyev, O.; Austin, A. J.; Cammi, R.; Pomelli, C.; Ochterski, J. W.; Martin, R. L.; Morokuma, K.; Zakrzewski, V. G.; Voth, G. A.; Salvador, P.; Dannenberg, J. J.; Dapprich, S.; Daniels, A. D.; Farkas, Ö.; Foresman, J. B.; Ortiz, J. V.; Cioslowski, J.; Fox, D. J. Gaussian, Inc.: Wallingford, CT, 2010.

(22) Mayer, I.; Salvador, P. *Chem. Phys. Lett.* **2004**, *383*, 368.

(23) The Becke's fuzzy atoms weights calculated using the minimum of the electron density along the interatomic distance to define the radio between the atomic radii of the two atoms, which is to be used in the Becke formula for calculating the weight functions.

(24) Becke, A. D. *J. Chem. Phys.* **1988**, *88*, 2547. Matito, E.; Solà, M.; Salvador, P.; Duran, M. *Faraday Discuss.* **2007**, *135*, 325.

(25) Mayer, I.; Salvador, P. Program "FUZZY", Version 1.00, Girona, Oct 2003.

(26) Reed, A. E.; Curtiss, L. A.; Weinhold, F. *Chem. Rev.* **1988**, *88*, 899.

(27) (a) Bickelhaupt, F. M.; Baerends, E. J. *Rev. Comput. Chem.* **2000**, *15*, 1. (b) Velde, G. T.; Bickelhaupt, F. M.; Baerends, E. J.; Guerra, C. F.; Van Gisbergen, S. J. A.; Snijders, J. G.; Ziegler, T. *J. Comput. Chem.* **2001**, *22*, 931.

(28) ADF2012, S., *Theoretical Chemistry*; Vrije Universiteit; Amsterdam, The Netherlands, <http://www.scm.com>.

(29) Becke, A. D. *J. Chem. Phys.* **1993**, *98*, 1372.

(30) (a) Chong, D. P.; Van Lenthe, E.; Van Gisbergen, S.; Baerends, E. J. *J. Comput. Chem.* **2004**, *25*, 1030. (b) Van Lenthe, E.; Baerends, E. J. *J. Comput. Chem.* **2003**, *24*, 1142.

(31) (a) Henkelman, G.; Jonsson, H. *J. Chem. Phys.* **2000**, *113*, 9978. (b) Crehuet, R.; Field, M. J. *J. Chem. Phys.* **2003**, *118*, 9563.

(32) Field, M. J. *J. Chem. Theory Comput.* **2008**, *4*, 1151.

(33) Stewart, J. J. P. *J. Mol. Model.* **2007**, *13*, 1173.

(34) It is important to remark that the PhF<sub>2</sub> and PhF<sub>3</sub> groups in the Hückel conformation are aligned in the perpendicular direction of the porphyrin rings, i.e., their steric effect is smaller than one can initially consider (see Figure S1 of the Supporting Information).

(35) By playing with the orientation of the OH and NH<sub>2</sub> groups, several Hückel conformations of the expanded porphyrin can be obtained. The H<sub>1</sub> structure has been selected, which implies the smallest rotational energy barriers of the porphyrin ring.

(36) (a) Jackson, A. H.; Kenner, G. W.; Smith, K. M. *J. Am. Chem. Soc.* **1966**, *88*, 4539. (b) Jackson, A. H.; Kenner, G. W.; Smith, K. M. *J. Chem. Soc. C* **1968**, 302. (c) Balch, A. L. *Coord. Chem. Rev.* **2000**, *200–202*, 349. (d) Khoury, R. G.; Jaquinod, L.; Paolesse, R.; Smith, K. M. *Tetrahedron* **1999**, *55*, 6713.

(37) The M05-2X functional has not been implemented in ADF yet, and for this reason, we have used the BH&HLYP functional for the EDA calculations.

(38) Fernández, I.; Frenking, G. *Faraday Discuss.* **2007**, *135*, 403.